·Article·
Advances in Polar Science
doi: 10.3724/SP.J.1085.2013.00175
September 2013 Vol. 24 No. 3: 175-182

Auroral event detection using spatiotemporal statistics of local motion vectors

WANG Qian[1,2*], LIANG Jimin[3] & HU Zejun[2]

[1] Image and Information Processing Research Center, Xi'an University of Posts and Telecommunications, Xi'an 710121, China;
[2] SOA Key Laboratory for Polar Science, Polar Research Institute of China, Shanghai 200136, China;
[3] Life Sciences Research Center, School of Life Sciences and Technology, Xidian University, Xi'an 710071, China

Received 12 May 2013; accepted 26 July 2013

Abstract The analysis and exploration of auroral dynamics are very significant for studying auroral mechanisms. This paper proposes a method based on auroral dynamic processes for detecting auroral events automatically. We first obtained the motion fields using the multiscale fluid flow estimator. Then, the auroral video frame sequence was represented by the spatiotemporal statistics of local motion vectors. Finally, automatic auroral event detection was achieved. The experimental results show that our methods could detect the required auroral events effectively and accurately, and that the detections were independent on any specific auroral event. The proposed method makes it feasible to statistically analyze a large number of continuous observations based on the auroral dynamic process.

Keywords **automatic detection, auroral event, fluid flow**

Citation: Wang Q, Liang J M, Hu Z J. Auroral event detection using spatiotemporal statistics of local motion vectors. Adv Polar Sci, 2013, 24:174-181, doi: 10.3724/SP.J.1085.2013.00174

1 Introduction

Changeable auroral morphology maps solar-terrestrial physics along the Earth's magnetic field lines projected onto the polar ionosphere. Much has been learned about the ionosphere and magnetosphere from auroral events[1]. The analysis of auroral mechanisms is very significant for studying auroral phenomena and their relationship with magnetospheric dynamics. The all-sky imaging system provides auroral data with spatial and temporal high-resolution. Since the Chinese Arctic Yellow River Station(YRS) started winter auroral observations in December 2003, they have obtained annually over 1 200 h of auroral observation images by all-sky imagers(ASI) at the YRS, assembled from three wavelengths (427.8, 557.7, and 630.0 nm).

The quantity of observational data from YRS has increased gradually by more than 1 million all-sky images per year, whereas the quantity of data from the THEMIS project is up to 10 million a year[2]. Therefore, exploring a way in which to analyze these data automatically and make full use of the large number of ASI images is becoming increasingly urgent for auroral researchers.

In our previous study, we analyzed automatically the static features of auroral phenomena using techniques of image processing and pattern recognition[3]. However, for various and complicated auroral phenomena, it is not sufficient to consider only the morphological characteristics of aurora phenomena. Thus, the analysis and exploration of auroral dynamic processes are very significant for studying auroral mechanisms. The occurrence and evolution of aurora are subject to various kinds of unknown factors resulting in extremely complex auroral motion. Therefore, many traditional technologies based on a certain assumption and model cannot accomplish auroral dynamic analysis. Most existing analysis of dynamic processes involves manual case studies of a very small number of auroral video frame sequences[4-5]. Therefore, the results obtained are difficult to apply in general. To make the results more

* Corresponding author (email: xinrzhsh24@126.com)

reliable and universal, an automatic analysis technology that analyzes auroral dynamic processes statistically, based on a large number of continuous observations of auroral sequences, is urgently needed.

Useful moving information for complex vision analysis can be obtained from the local motion field. Blixt et al.[6] estimated the global auroral two-dimensional motion field using a robust optical flow field and studied the validity of this method for auroral data. However, some questions arise from their work. First, optical flow field technology is based on an assumption of brightness constancy, for which the brightness of the observed object remains constant during motion. In classical computer vision research, we usually assume that moving objects are rigid and that their features are stable and prominent. However, there is no such thing as an "object" in most auroral images. In the evolution process, deformation of auroral morphology will occur, and combination or division of auroral structures will happen. Furthermore, an aurora is the effect caused by highly energetic charged particles colliding with the atmosphere within an extremely short time; thus, the brightness constancy assumption is not feasible for auroras. Second, when solving the optical flow field, the solution of the target equation is apparent velocity denoted as its differential form. The velocity-based underlying assumption is that the motion velocity of an image series is very small owing to the differential property. However, in the evolution of auroras, extremely energetic movements often occur, especially when substorms occur. Third, the data used were auroral video frame sequences with a narrow view. This creates another very serious problem regarding discontinuous motion and boundaries in the process of calculating the optical flow field. Auroral structure may move out view of subsequent auroral images, resulting in no matching parts among image sequences at the motion boundaries.

The most important issue for motion analysis of the optical flow field is how to use the local motion field to represent the moving features of multiframe sequences. In previous research[7-9], Nelson and Polana adopted scale- and direction-based spatial statistics to classify a small number of moving images[7]. Based on this, Fablet and Bouthemy used the temporal and multiscale co-occurrence statistics to denote sequences[8]. However, in those two methods, neither spatiotemporal statistics nor features were fully represented. Considering the temporal and spatial features of dynamic texture motion simultaneously, Peh and Cheong constructed two individual maps for scale and direction[9]. Then, they processed the two maps separately as ordinary image texture, which will lose the moving two-dimensional information.

Given the non-rigid features of auroras, we introduced fluid flow to auroral image analysis[10]. The algorithm constructed models with continuity equations of fluid to obtain constraint equations of brightness. Thus, the size, direction, and distribution of the local motion vectors between two consecutive frames are obtained. Considering the randomness of auroral phenomena, in this paper, we propose spatiotemporal statistics of the local motion vector to represent the auroral video frame sequence. Using this representation, we measure the proximity between the concerned objective sequence and all auroral subsequence from the auroral database. Finally, a simple threshold operation is conducted to detect automatically multiple events, including polar motion, cloudy weather, and diffuse auroras.

2 Extraction of local motion fields

An aurora is a geophysical phenomenon generated by the collision between the atmosphere and highly energetic charged particles moving along the high-latitude magnetic lines. The brightness pattern of an auroral image is different from that of a traditional image analyzed through pattern recognition, because the aurora will deform, grow, and vanish. Because of the intrinsic factors of auroras, the traditional optical flow field analysis based on the brightness constancy assumption cannot be applied to estimate the auroral motion field. Therefore, the fluid flow method is introduced to overcome this problem.

The fluid flow method used in this paper was proposed by Corpetti et al. in 2002 to estimate the movement of atmospheric images[10]. There are two reasons why we choose it to estimate auroral motions. First, the motion is constructed by continuity equations, which are derived from the laws of conservation of mass and momentum[10]. The equation is also applied extensively to the analysis of moving images, including water waves, atmosphere, and smoke. Second, this method uses an integral form of brightness constraint, and data constraint is represented as an integral form at different spatial resolutions. This means that the solution of the objective function is the displacement of auroral motion, and that the auroral large-scale movement problem will be effectively settled.

The auroral data used in this paper were obtained from the all-sky imagers at YRS, Ny-Alesund, Svalbard. YRS is located at 78.92°N, 11.93°E, and corrected geomagnetic latitude 76.24°N, where MLT=UT+3.1 h. Four ASI images are shown in Figure 1. Theoretically, ASI images contain all the information above the horizon, and the brightness relationship between the all-sky auroral images and that within a zenith angle of 80° is linear; therefore, the auroral structure of concern occurs within the above region. With the auroral images with a narrow horizon used by Blixt et al.[6], the structure of concern of an independent auroral event will move out of subsequent image frames. However, this problem can be circumvented using ASI images. Moreover, the continuity equation of brightness constraint is based on the assumptions of global variation and momentum conservation[10]. Therefore, the all-sky image is much better than the auroral image with a narrow horizon for ensuring validity of the assumption of fluid flow.

The performance of auroral image analysis between classical optical flow field and fluid flow field are compared in this article. The first algorithm includes a global constraint algorithm proposed by Horn-Schunck (HS)[11]

and a local constraint algorithm proposed by Lucas-Kanade (LK)[12]. To estimate the validity of fluid in extracting motion features of various auroral video frame sequences, four types of consecutive auroral images are used, as shown in Figure 1. The superimposed red arrows on the all-sky images (Figure 1) denote the motion field using each of the three methods (HS, LK, and fluid flow).

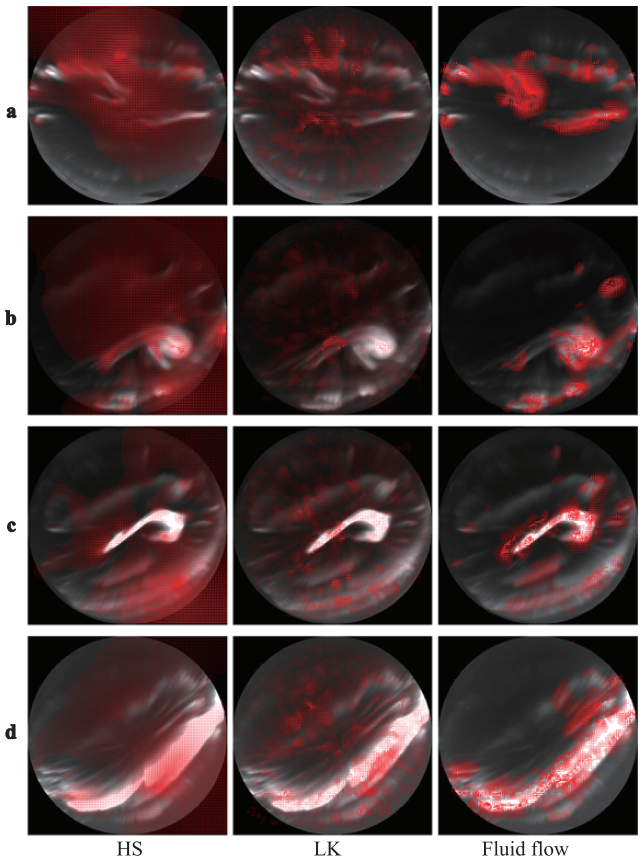

Figure 1 Motion fields of ASI images using three methods.

Apparently, the fluid flow method obtains better results in extracting auroral motions, whereas moving auroral motion patterns cannot be captured by LK and HS. We attribute this failure to three causes: Brightness conservation is no longer useable, large auroral motion is beyond the limit of the differential equations, and the motion of neighboring pixels is dissimilar, which is contrary to the requirement of the smoothing regularization. Non-rigid features, deformation, and translucence may be the cause for the failure of traditional methods.

3 Spatiotemporal statistics of local motion fields

An auroral video frame sequence is denoted as $S=\{s(\boldsymbol{x},t), \boldsymbol{x}\in\boldsymbol{D}, t=1,2,\cdots,T\}$, where $\boldsymbol{D}$ represents the spatial region and T indicates the length of the sequence. With the fluid flow method referred to in section 1, the local motion vector $\{\boldsymbol{v}(\boldsymbol{x}, t), \boldsymbol{x}\in\boldsymbol{D}, t=1,2,T-1\}$, which contains all motion vectors within the $\{\boldsymbol{D}\times T\}$ spatiotemporal domain, is obtained. The two-dimensional vector field $\boldsymbol{V}$ is projected onto a two-dimensional polar coordinate plane $\boldsymbol{P}$, which is pre-segmented into n regions $\{r_i, i=1,\cdots, n\}$. First, we calculate, in the space-time domain, the number of all vectors that were projected onto every region r_i of $\boldsymbol{P}$, and the histogram of each vector can be obtained. Then, the histograms are normalized to obtain $H=\{h_1, h_2,\cdots, h_n\}$. The histogram represents the two-dimensional statistical distribution of all vectors of spatiotemporal region $\{\boldsymbol{D}\times T\}$ and a comparison between two sequences with different lengths can be achieved through normalization. These processes are shown in Figure 2. The polar coordinate plane is nonlinearly divided into eight ranges in amplitude [0.1, 0.2, 0.5, 1, 3, 5, 8, 12, $+\infty$] and four ranges by orientation [−135°, −45°, 45°, 135°]. Following many experiments, it has been determined that these parameters achieve the best performance.

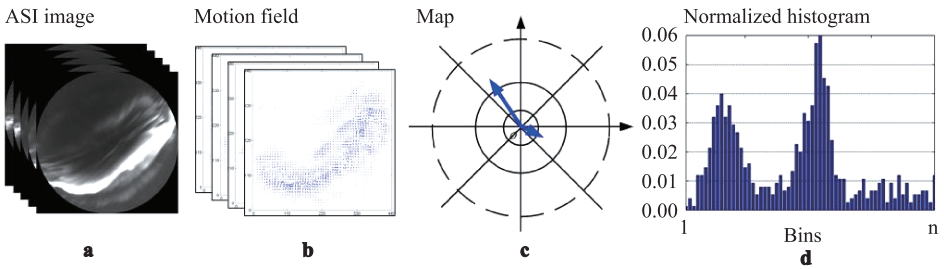

Figure 2 Scheme of building spatiotemporal statistical representation of local vector for the ASI image. **a**, ASI images; **b**, local motion fields; **c**, map; **d**, normalized histogram.

4 Detecting auroral events

To study the time of auroral occurrence and the pattern of auroral movement, we need to find some particular and similar auroral events from very long auroral video frame sequences as quickly as possible. Local motion vector-based spatiotemporal statistics can represent arbitrary subsequences of an auroral video frame sequence and they can be used to calculate the similarity between two auroral video frame sequences of different lengths. First, we choose an auroral event as an objective event and compare it with all subsequences in the database. Events with greater similarity than a predetermined threshold value are deemed similar auroral events.

The so-called objective event is an auroral video frame sequence with size, and its corresponding spatiotemporal statistical characteristics f_1, based on local vectors, can be acquired from the method mentioned in section 2. Similar auroral events are retrieved among auroral video frame sequence S_2 with length $L(L \gg 1)$. To locate similar sequences accurately, a sliding window with size T is used on S_2 and the size for each step is 1, which means there is an overlap between the sliding windows. Based on the local motion field, spatiotemporal statistics of auroral video frame sequence S_2^i of sliding window i is represented as f_2^i. Distance χ^2 measures the distance between objective event S_1 and auroral video frame sequence S_2^i of sliding window i. Here, distance χ^2 is written as:

$$\chi^2(p,q) = \Sigma_i \ (p_i - q_i)2 \ /(p_i - q_i) \tag{1}$$

where i indicates the index of the feature vector. Based on (1), the similarity between two sequences is defined as:

$$s_{\text{ind}}(i) = \exp\left(-\frac{\chi^2(f_1, f_2^i)}{\sigma}\right). \tag{2}$$

The similarity measurement is obtained from the difference using the normal distribution function (positive axie) nonlinearly, where determines the scale of the normal distribution function. The greater $s_{\text{ind}}(i)$ is, the more similar the objective event and the subsequences constituted by the -th frame and next continuous $T-1$ frames of S_2 are. Auroral events, when s_{ind} is greater than the threshold value, are deemed similar auroral events, detected by selecting an appropriate threshold value.

To achieve the detection operation above, we must set the size of the sliding window and the threshold value. To represent completely the auroral motion pattern and to reduce the influence of noise as much as possible, the length of the auroral video frame sequence to be compared cannot be set too large. However, to locate accurately the beginning and end time of similar events, the length cannot be set too small. Therefore, it is necessary to consider both the extent of activity and duration of the objective event when setting the size of the sliding window.

5 Experimental results

5.1 Results of detecting auroral poleward-moving feature

The auroral observations studied in this paper were obtained from the all-sky imagers at YRS from December 2003 to January 2004, including an observation period of 20 d. A poleward-motion event is selected as the objective event. An auroral poleward-moving feature is related to many special geomagnetic physical phenomena[13]; thus, the study of such features is very important. Our goal is to detect the auroral events moving towards high latitudes. Here, the poleward-motion event detected in this paper is different from the poleward-moving auroral form of auroral morphology, which also includes other auroral forms possessing features with poleward motion.

Apparent poleward motion of auroral arcs occurred during 12:44−12:55 UT on 25 December 2003. In the Keogram[1], an auroral emission region moved quickly from −60° to +60° (Figure 3). We selected the auroral video frame sequence that occurred during 12:44−12:55 UT on 25 December 2003 as objective event 1, and then attempted to detect similar events from the 2003 to 2004 observations. The curve of similarity between objective event 1 and auroral activities during 03:00–15:00 UT on 1 January 2004 is represented in Figure 4a, where σ, T, and the threshold value are 0.075, 20, and 0.88, respectively. Figure 4b is the corresponding Keogram. The red labels at the top of the figure indicate the occurrence of poleward motion labeled manually, and the orange labels at the bottom represent similar events detected automatically. As can be seen from Figure 4b, the aurora occurring at the labeled time did indeed move towards magnetic north. A sequence of ASI images (04:48:31–05:02:21 UT) is shown in Figure 5. The aurora in Figure 5 displays a similar motion tendency to that in Figure 3.

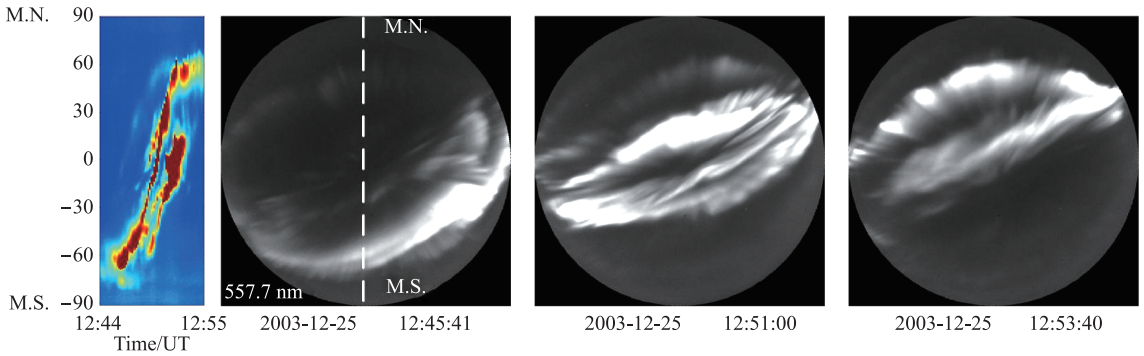

Figure 3 Keogram and three ASI images of poleward-moving auroral event during 12:44–12:55 UT on 25 December 2003. M.N. and M.S. denote magnetic north and magnetic south, respectively.

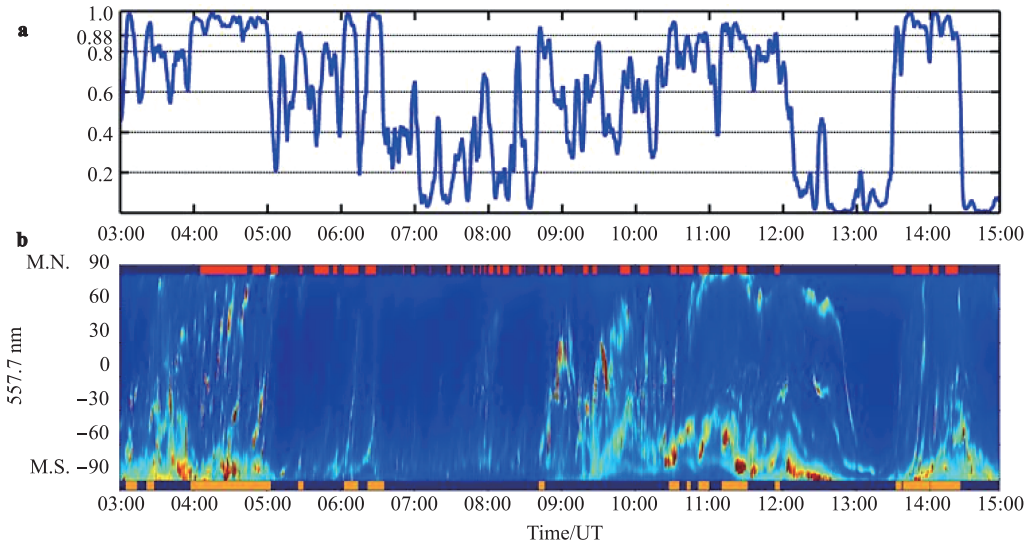

Figure 4 Poleward-moving auroral event detected at 03:00–15:00 UT on 1 January 2004. **a**, similar curve between auroral activities and objective event 1; **b**, keogram and labels of detected similar events.

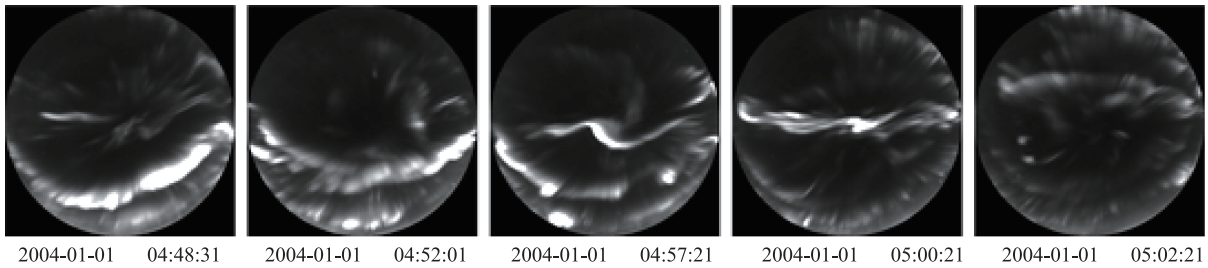

Figure 5 ASI images at 04:48:31–05:02:21 UT on 1 January 2004.

By comparing the orange labels with the red ones, it can be seen that the results of the automatic detection are similar to the manual labeling. The rate of accuracy is up to 84.3% and the corresponding recall of detection is 71.8%. The biggest difference between the two labels occurs at 07:00–08:00 UT. We attribute this difference to using only the data at 557.7 nm in the automatic detection, whereas we observed data in three wavelengths (427.8, 557.7, and 630.0 nm) for the manual labeling process. The emissions at 557.7 nm are too weak to detect the poleward motion during 07:00–08:00 UT in Figure 4b, whereas the emissions at 630.0 nm in the Keogram exhibit obvious characteristics of poleward movement.

In addition to the results shown in Figure 4, Keograms at 557.7 nm on 22 December 2003, 18 January 2004, and 23 January 2004 are shown in Figure 6. The red labels at the top of the figure are the manual labels, and the orange labels at the bottom are the labels of poleward-moving auroral events detected automatically. A comparison of the rate of accuracy and the recall of detection is shown in Table 1, and the mean values of the four days are 82.0% and 79.4%. The features of auroral poleward motion on 23 January 2004 are accurately detected and the corresponding recall of detection is 81.7%. The auroral events labeled by the orange labels are very different from each other in brightness, appearance, complexity, and event length, which signify that our method is robust against the differences in duration of event, auroral appearance, and velocity of auroral movement. There are three reasons why the method detects the location of similar auroral events successfully. First, the detection is based on moving auroral features rather than auroral brightness, morphology, distribution, and location. Second, the nonlinear statistics of auroral motion vectors and the appropriate partitioning of the polar coordinate plane ensure that the method can detect moving auroras with different velocities. Finally, in this paper, we compute the spatiotemporal statistics of an entire volume of a sequence, without concern for the exact locations of the motion vectors.

5.2 Evaluation of multiple objective events

The detection above is based on objective event 1, which possesses obvious poleward-moving features and relatively simple motion. However, there are changes, during the active period, in the motion velocity, duration, and structure of the aurora. In this section, we select multiple events that are similar in motion tendency, but different in active period, motion velocity, duration, and auroral structure. These events are selected as objective events to detect similar events. The detected results will be compared to evaluate

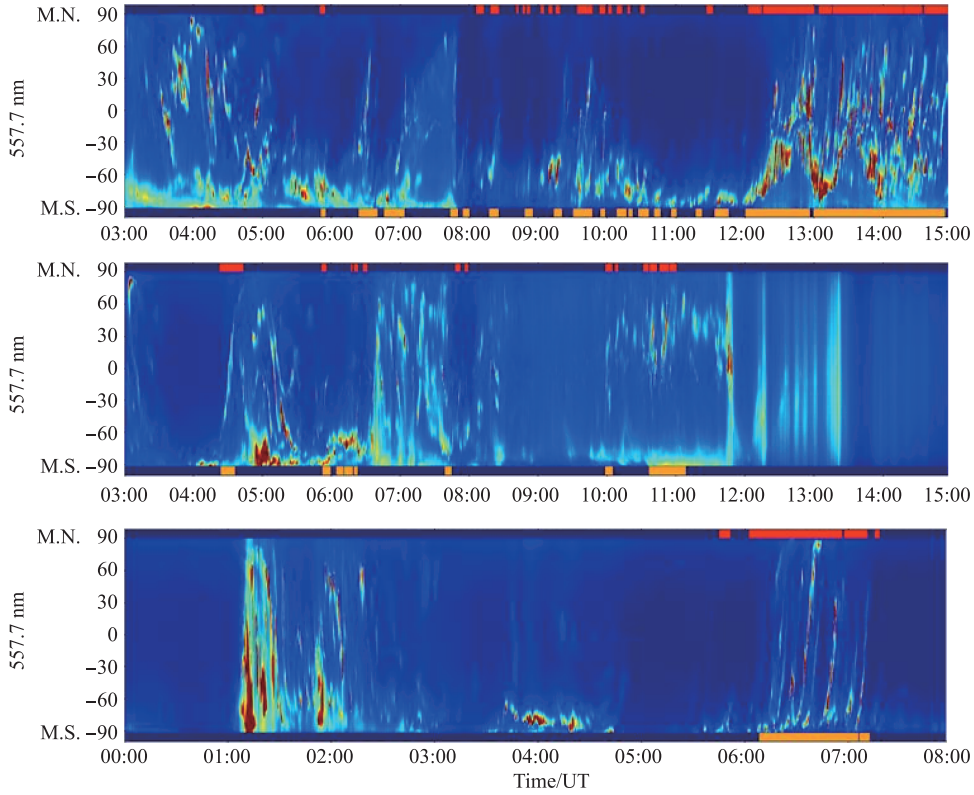

Figure 6 Detected poleward-moving auroral forms on 22 December 2003, 18 January 2004, and 23 January 2004.

Table 1 Rate of accuracy and recall of detection on 22 December 2003, 1 January 2004, 18 January 2004, and 23 January 2004

	Detecting data				Average accuracy
	2003-12-22	2004-01-01	2004-01-18	2004-01-23	
Rate of accuracy /%	73.6	84.3	70.1	100.0	82.0
Recall of detection /%	92.1	71.8	72.1	81.7	79.4

the impact and dependency of the choice of objective events on the detection results.

Four auroral events that all possess poleward-moving features are selected as objective events. The Keograms and ASI images of objective event 2 (21 December 2003), 3 (24 December 2003), 4 (30 December 2003), and 5 (14 January 2004) are shown in Figure 7. We detect similar events in the auroral observations from 2003 to 2004. The Keograms show that all four objective events possess obvious poleward-moving features, but that they are different to each other in two-dimensional morphological characteristics in the ASI images, activity period, motion velocity, and duration time.

As shown in Figures 8–10, the detected locations of the four lines, labeled in orange, are similar. For several important events, such as the events occurring at 4:30 UT on 18 January 2004 and from 6:00 to 7:00 UT on 23 January 2004, the detection labels are very similar and accurate. The major differences lie in the labels of brief auroral activity. By statistical analysis, the duration time of those brief auroral activities is no more than 460 s. The experimental results demonstrate that the proposed method can achieve

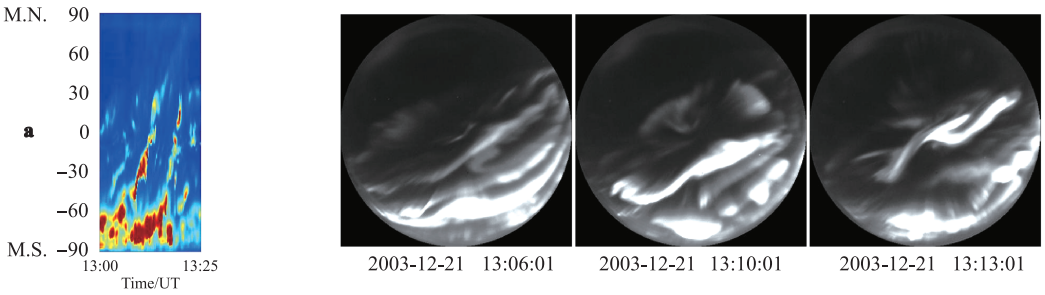

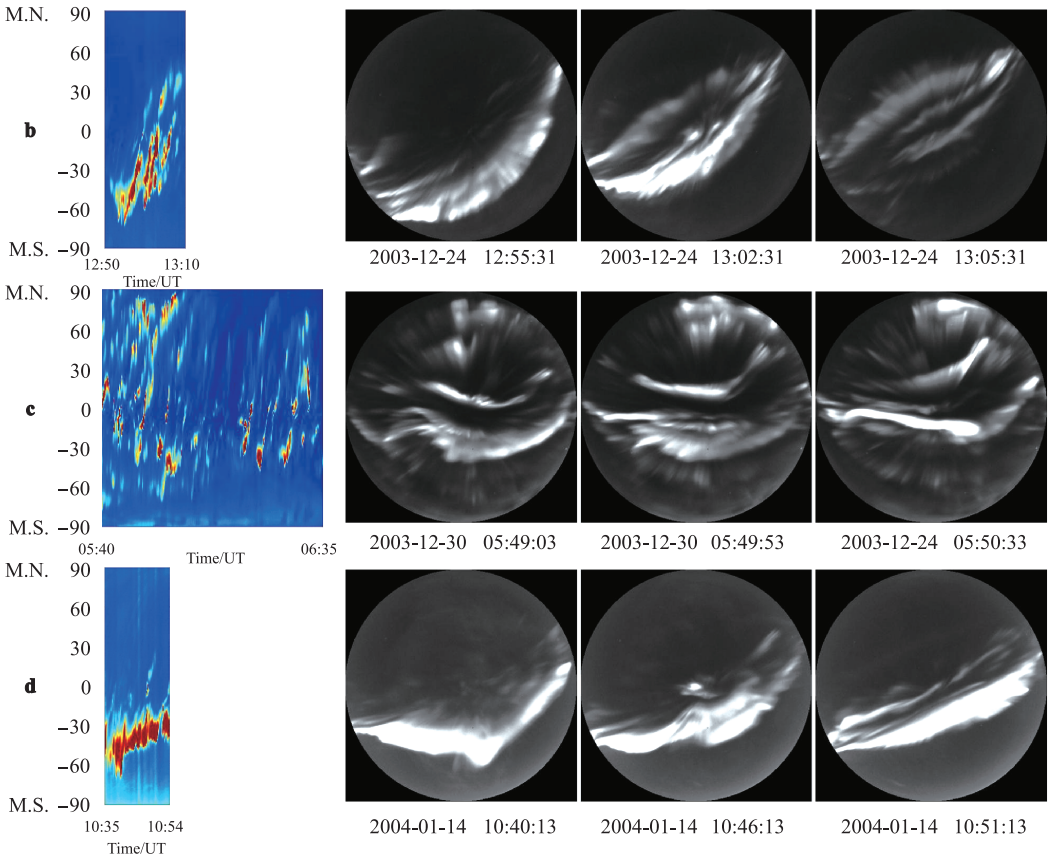

Figure 7 Keograms and ASI images of objective events 2, 3, 4, and 5.

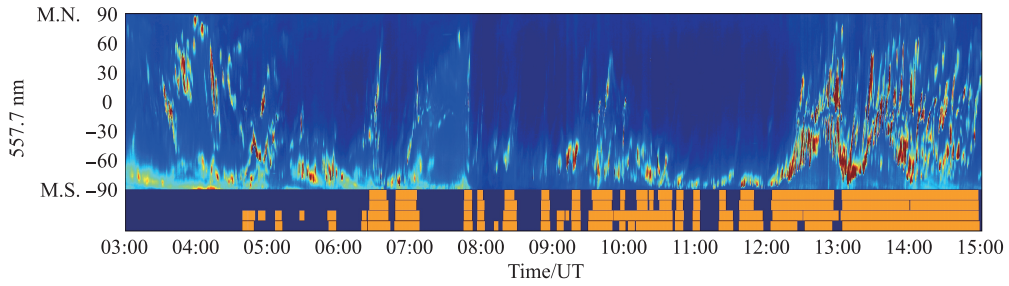

Figure 8 Detected poleward-moving auroral features on 22 December 2003 by using objective events 2, 3, 4, and 5.

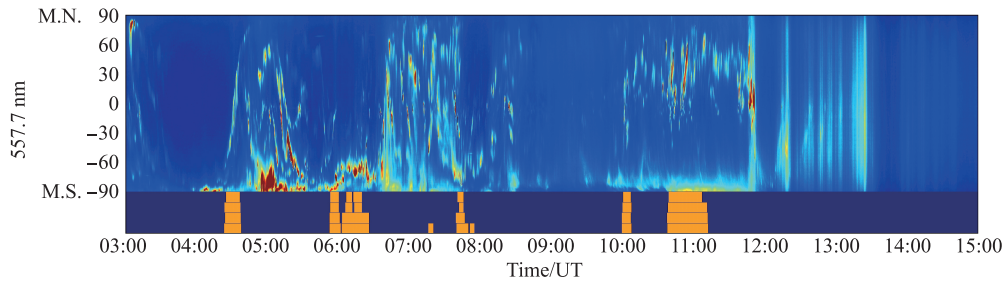

Figure 9 Detected poleward-moving auroral features on 18 January 2004 by using objective events 2, 3, 4, and 5.

automatic detection of poleward-moving features, robustly and stably, without dependence on the choice of objective events. It is noteworthy that not only can it detect poleward-moving features, but our method could also detect any auroral activities with any apparent direction of motion.

6 Conclusions

Dynamic information is one of the most important characteristics for analyzing image sequences. In this study, we

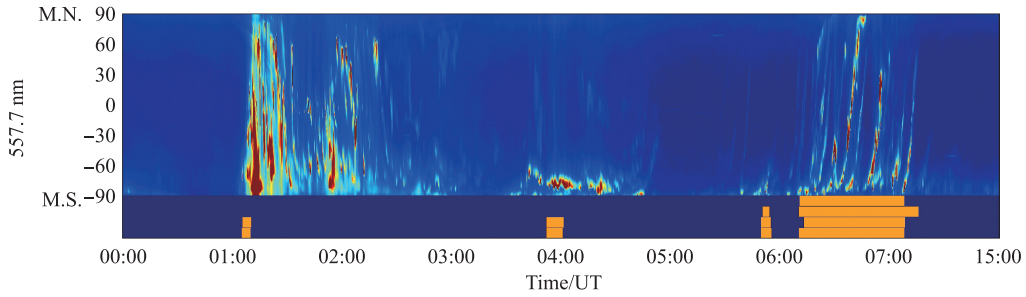

Figure 10 Detected poleward-moving auroral features on 23 January 2004 by using objective events 2, 3, 4, and 5.

concentrate on researching features of auroral motion and propose a representation method for auroral ASI image sequences based on fluid flow. The fluid flow method is not based on the brightness constancy assumption. The motion fields estimated by using fluid flow provide the underlying information for analyzing auroral events. Because of the diversity and randomness of auroral activities, we compute the spatiotemporal statistics of local vectors for a sequence. Using this representation, we can measure the similarity between two auroral video frame sequences with different lengths. The detection of auroral events is thereby achieved, which establishes a foundation for achieving statistical analysis of auroral image sequences.

As a preliminary effort towards applying image processing and pattern recognition techniques to detect auroral events, our research is far from complete. Several problems need further investigation. First, the detection results rely on a single auroral event. Fusion of the results from multiple detections appears a promising solution for improved recall rate. Second, the objective event and the observations detected are from the ASI imager from the same year and location. In future studies, we will use various data to evaluate our methods further. Finally, because of the use of the fisheye lens, there are deformations on the boundaries of the ASI image; therefore, we will conduct geometric calibration for the estimated motion fields.

Acknowledgments This research is supported by the National Natural Science Foundation of China(Grant nos. 41274164, 41031064), the Ocean Public Welfare Scientific Research Project of China(Grant no. 201005017), the Foundation of Shaanxi Educational Committee(Grant no. 12JK0543), and the Youth Research Project of the Xi'an University of Posts and Telecommunications(Grant no. ZL2012-01). Data were issued by the Data-sharing Platform of Polar Science (http://www.chinare.org.cn) maintained by Polar Research Institute of China (PRIC) and Chinese National Antarctic & Arctic Data Center(CN-NADC).

References

1 Hu Z J, Yang H G, Huang D H, et al. Synoptic distribution of dayside aurora: Multiple-wavelength all-sky observation at Yellow River Station in Ny-Ålesund, Svalbard. Journal of Atmospheric and Solar-Terrestrial Physics, 2009, 71(8-9): 794-804, doi: 10.1016/j.jastp.2009.02.010.

2 THEMIS project. http://aurora.phys.ucalgary.ca/themis/themis_main.html.

3 Wang Q, Liang J M, Hu Z J, et al. Spatial texture based automatic classification of dayside aurora in all-sky images. Journal of Atmospheric and Solar-Terrestrial Physics, 2010, 72(5-6): 498-508.

4 Sandholt P E, Farrugia C J, Denig W F. Dayside aurora and the role of IMF $|B_y|/|B_z|$: detailed morphology and response to magnetopause reconnection. Annales Geophysicae, 2004, 22(2): 613-628.

5 Sandholt P E, Dyrland M, Farrugia C J. Dayside aurorae and polar arcs under south-east IMF orientation. Annales Geophysicae, 2006, 24: 3421-3432.

6 Blixt E M, Semeterand J, Ivchenko N. Optical flow analysis of the aurora borealis. Geoscience and Remote Sensing Letters, IEEE, 2006, 3(1): 159-163.

7 Nelson R C, Polana R. Qualitative recognition of motion using temporal texture. CVGIP: Image Understanding, 1992, 56(1): 78-89.

8 Fablet R, Bouthemy P. Motion recognition using nonparametric image motion models estimated from temporal and multiscale co-occurrence statistics. IEEE Transactions on Pattern Analysis and Machine Intelligence, 2003, 25(12): 1619-1624.

9 Peh C H, Cheong L F. Synergizing spatial and temporal texture. IEEE Transactions on Image Processing, 2002, 11(10): 1179-1191.

10 Corpetti T, Memin E, Perez P. Dense estimation of fluid flows. IEEE Transactions on Pattern Analysis and Machine Intelligence, 2002, 24(3): 365-380.

11 Horn B K P, Schunck B G. Determining optical flow. Artificial Intelligence, 1981, 17(1-3): 185-203.

12 Lucas B D, Kanade T. An iterative image registration technique with an application to stereo vision// Proceedings of the International Joint Conference on Artificial Intelligence 1981. San Francisco, CA: Morgan Kaufmann Publishers, 1981.

13 Sandholt P E, Farrugia C J. Role of poleward-moving auroral forms in the dawn-dusk auroral precipitation asymmetries induced by IMF B_y. Journal of Geophysical Research, 2007, 112: A04203.